FULL PAPER

Dalton
www.rsc.org/dalton

Synthesis and properties of $[M^{II}(L^6)_2][ClO_4]_2$ (M = Fe, Co and Ni): structures of Co and Ni complexes and spin-state transition by Fe complex (L^6 = 2-[3-(2′-pyridyl)pyrazol-1-ylmethyl]-pyridine) †

Shubha Singh, Vibha Mishra, Jhumpa Mukherjee, N. Seethalekshmi and Rabindranath Mukherjee *

Department of Chemistry, Indian Institute of Technology, Kanpur-208 016, India.
E-mail: rnm@iitk.ac.in

Received 19th May 2003, Accepted 8th July 2003
First published as an Advance Article on the web 28th July 2003

A new non-planar tridentate ligand 2-[3-(2′-pyridyl)pyrazol-1-ylmethyl]pyridine (L^6) and its mononuclear bis-ligand complexes $[M(L^6)_2][ClO_4]_2$ [M = Fe (**1**), Co (**2**) and Ni (**3**)] have been synthesized. In the dications of six-co-ordinate complexes of **2** and **3**, each L^6 is arranged in a meridional mode. Structural analyses reveal that the $M–N_{pyrazole}$ bond length is appreciably shorter than the $M–N_{pyridine}$ bond lengths. Due to the weak field nature of L^6 (absorption spectral analyses) towards Fe(II), Co(II) and Ni(II) the complexes are uniformly high-spin at room-temperature. Temperature-dependent magnetic susceptibility measurements reveal that while Co(II) and Ni(II) complexes remain high-spin over the entire range investigated (6–300 K for **2** and 63–300 K for **3**), the Fe(II) complex exhibits a temperature-induced (5.2–300 K) spin transition in going from the $S = 2$ state at 300 K to predominantly an $S = 0$ state below 80 K. From the linear ln K_{eq} [$^1A_1$ (ls) ↔ $^5T_2$ (hs)] *vs.* $1/T$ relationship (190–250 K) the derived thermodyanamic parameters are: $\Delta H = 9.7 \pm 0.04$ kJ mol^{-1} and $\Delta S = 56 \pm 0.18$ J K^{-1} mol^{-1}. While complex **1** displays in MeCN an irreversible M^{III}/M^{II} redox process [anodic peak potential, $E_{pa} = 1.06$ V *vs.* SCE], for complex **2** such a redox process is reversible [$E_{1/2} = 0.74$ V *vs.* SCE and $\Delta E_p = 80$ mV].

Introduction

Pyridine derivatives are among the most versatile and thoroughly studied groups of ligands in co-ordination chemistry. Pyrazoles are arguably the most easily derivatised N-heterocycles and therefore readily afford a large variety of pyrazolylpyridine-based chelating ligands.[1–4] The co-ordination chemistry of pyrazole-derived chelating ligands,[1a] in addition to well known tris(pyrazolyl)borates,[1b] has vigorously developed. During the past decade we have investigated the co-ordination chemistry using non-planar bi- and tri-dentate heterocyclic ligands (L^1–L^5) to control the stereochemistry at metal(II) centres.[5–9] The ligand 2,6-bis(pyrazol-1-ylmethyl)pyridine (L^3) forms co-ordination compounds with transition metal ions, including bis-ligand iron(II) complex which undergoes temperature-induced spin transition. In the bis-ligand complexes the metal ion is surrounded by four pyrazole and two pyridyl groups, with electronic communication between pyrazole and pyridyl rings prevented due to the presence of methylene spacers. Many of such complexes have been structurally characterized by us[8] and others[10,11] to reveal that the ligand molecules are not planar, the pyridyl and pyrazole rings being twisted relative to each other. Following our investigations into the co-ordination behaviour of the L^1–L^5 ligands, it became clear that it would be valuable to extend this class of non-planar heterocyclic ligands. As a first step in a search for new such systems we have directed attention to the derivative of L^1.

While the pyridine unit in the versatile mixed-heterocycle synthon/ligand 3-(2-pyridyl)pyrazole[12–16] has strong π-accepting ability and consequently provides a soft site for metal co-ordination, the pyrazole unit is a better π donor and acts as a hard donor site. Hence, owing to the presence of this combination of soft and hard sites in a single heterocyclic system, a fine tuning of the physical and chemical properties of the metal complexes of such ligands might be attainable. Moreover, if to this 3-(2-pyridyl)pyrazole unit conformational flexibility is imposed, for instance by having a methylene spacer between this unit and a pyridine moiety as in L^6, such a ligand could permit several different co-ordination modes. In this contribution, we describe the synthesis and co-ordination behaviour of a new non-planar ligand 2-(3-(2′-pyridyl)pyrazol-1-ylmethyl)pyridine (L^6), towards bivalent first-row transition-metal ions (Fe, Co, Ni). Hoping that attachment of a pyridyl group to the 3-position of the pyrazole ring of 2-(pyrazol-1-ylmethyl)-pyridine (L^1) would provide an additional pyridyl co-ordination to the metal centre and in turn in its bis-ligand complexes metal ion would experience the crystal field of four pyridyl and two pyrazole groups. This situation is not simply the reverse of that observed with bis-ligand complexes of L^3–L^5: in addition two of the pyridyl rings and the two pyrazole rings are now capable of communicating electronically. This is the first example of such an endeavour and accordingly we were interested to see whether this apparently small modification of the parent ligand L^1 would lead to significant differences in the molecular structural, absorption spectroscopic, spin-state and redox properties of the resulting complexes. Here we describe results of such an investigation.

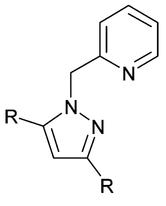

R = H, L^1
R = Me, L^2

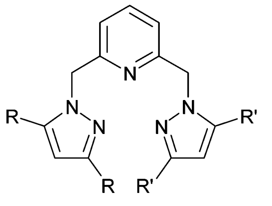

R = R' = H, L^3
R = H, R' = Me, L^4
R = R' = Me, L^5

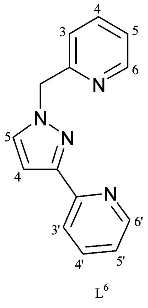

L^6

---

† Electronic supplementary information (ESI) available: Fig. S1–S6 discussed in the text. See http://www.rsc.org/suppdata/dt/b3/b305574d/

DOI: 10.1039/b305574d

Experimental

Reagents and materials

All chemicals were obtained from commercial sources and used as received. Solvents were purified/dried following standard procedures.[5–7,9,17] Tetra-*n*-butylammonium perchlorate (TBAP), was prepared/purified as before.[17] 3-(2-pyridyl)pyrazole was synthesized following a reported procedure[12b]

Syntheses

2-(3-(2′-pyridyl)pyrazol-1-ylmethyl)pyridine, L^6. A mixture of 2-picolyl chloride hydrochloride (0.985 g, 6.0 mmol), 3-(2-pyridyl)pyrazole (0.87 g, 6.0 mmol), benzene (75 cm^3), 40% aqueous NaOH (15 cm^3) and 40% aqueous tetra-*n*-butylammonium hydroxide (8 drops) was refluxed with stirring for 8 h and then stirred at room temperature overnight. The organic layer was then separated, dried over anhydrous Na_2SO_4 and filtered. Then the solvent was evaporated *in vacuo* to obtain a yellowish white solid (3.21 g, 97%). ^{1}H NMR (80 MHz; $CDCl_3$): δ 5.40 (2 H, s, CH_2), 6.89 (1 H, d, pyrazole H^4), 7.04 (3 H, m, py H^{3,4,5}), 7.57 (3 H, m, py H$^{3',4',5'}$), 7.90 (1 H, d, pyrazole H^5), 8.53 (2 H, two overlapping doublets, pyridine H^6 and H$^{6'}$).

$[Fe(L^6)_2][ClO_4]_2$ (1). To a stirred solution of L^6 (0.125 g, 0.520 mmol) in MeOH (4 cm^3), solid $[Fe(H_2O)_6][ClO_4]_2$ (0.096 g, 0.264 mmol) was added in small portions. After 15 min the bright yellow precipitate that formed was collected by filtration, washed with the minimum amount of MeOH and dried *in vacuo* (yield, 0.150 g, *ca.* 78%). Recrystallisation was achieved by diffusion of diethyl ether (10 cm^3) into an MeCN solution (4 cm^3) of the complex. Found: C, 46.77; H, 3.24; N, 15.92. Calc. for $C_{28}H_{24}N_8O_8Cl_2Fe$: C, 46.23; H, 3.30; N, 15.41%. Molar conductance, Λ_M (MeCN, 298 K) = 258 Ω^{-1} cm^2 mol^{-1} (expected range[18] for 1 : 2 electrolyte: 220–300 Ω^{-1} cm^2 mol^{-1}). UV/VIS (MeCN), λ_{max}/nm (ε/dm^3 mol^{-1} cm^{-1}): 809 (13), 409 (1150), 288 (21 500), 243 (26 200).

$[Co(L^6)_2][ClO_4]_2$ (2). To a stirred solution of L^6 (0.150 g, 0.635 mmol) in MeOH (4 cm^3), solid $[Co(H_2O)_6][ClO_4]_2$ (0.116 g, 0.317 mmol) was added in small portions. After 5 min the pink precipitate that appeared was collected by filtration, washed with the minimum amount of MeOH and dried *in vacuo* (yield, 0.120 g, *ca.* 52%). Diffraction quality single crystals were grown by diffusion of diethyl ether (10 cm^3) into an MeCN solution (4 cm^3) of the complex. Found: C, 45.94; H, 3.44; N, 14.95. Calc. for $C_{28}H_{24}N_4O_4Cl_2Co$: C, 46.03; H, 3.29; N, 15.34%. Molar conductance, Λ_M (MeCN, 298 K) = 255 Ω^{-1} cm^2 mol^{-1}. UV/VIS (MeCN), λ_{max}/nm (ε/dm^3 mol^{-1} cm^{-1}): 905 (12), 554 (sh) (26), 522 (30), 477 (34), 288 (21 100), 247 (27 800).

$[Ni(L^6)_2]$ $[ClO_4]_2$ (3). To a stirred aqueous (1 cm^3) solution of $[Ni(H_2O)_6][ClO_4]_2$ (0.153 g, 0.418 mmol) a solution of L^6 (0.200 g, 0.848 mmol) in MeOH (1 cm^3) was added. After 15 min an additional amount of MeOH (1 cm^3) was added and kept in air for slow evaporation. Within 24 h light violet coloured highly crystalline precipitate that formed was collected by filtration, washed with a minimum amount of MeOH and dried *in vacuo* (yield 0.2 g, *ca.* 65%). Single crystals suitable for structural studies were obtained from the filtrate. Found: C, 46.40; H, 3.40; N, 15.10. Calc. for $C_{28}H_{24}N_4O_4Cl_2Ni$: C, 46.02; H, 3.29; N, 15.34%. Molar conductance, Λ_M (MeCN, 298 K) = 246 Ω^{-1} cm^2 mol^{-1}. UV/VIS (MeCN), λ_{max}/nm (ε/dm^3 mol^{-1} cm^{-1}): 870 (38), 780 (sh) (22), 558 (23), 290 (19 100), 245 (25 400).

Caution: perchlorate salts of compounds containing organic ligands are potentially explosive.

Physical measurements

Elemental analyses (C, H, N) were obtained at the Microanalysis Service Centre at this Department. Infrared spectra were recorded on a Brüker Vector 22 spectrophotometer using KBr discs. Electronic spectra were recorded either using a Perkin Elmer Lambda 2 or Agilent 8453 diode-array spectrophotometer. Solution electrical conductivity measurements (25 °C) were carried out with an Elico (Hyderabad, India) Type CM-82 T conductivity bridge.

Magnetism

For **1** and **2** variable temperature magnetic susceptibility measurements were obtained in the solid state using a Quantum Design (Model MPMSXL-5) SQUID magnetic susceptometer operating at magnetic fields of 1.5 and 0.5 T, respectively. Variable temperature (63–300 K) magnetic susceptibilities measurements on **3** in the solid state were performed using a locally-built Faraday balance[19] comprising an electromagnet with constant gradient pole caps (Polytronic Corporation, Mumbai, India), an ultravacuum Sartorius M25-D/S Balance (Germany), a closed-cycle refrigerator and a Lake Shore temperature controller (Cryo Industries, USA). All measurements were made at a fixed main field strength of ~0.6 T. Magnetic susceptibility measurements in MeCN solution were obtained by Evans's method[20] using a PMX-60 JEOL (60 MHz) NMR spectrometer. Susceptibilities were corrected for diamagnetic contributions for the sample, by using literature values.[21] Effective magnetic moments were calculated from $\mu_{eff} = 2.828 [\chi_M T]^{1/2}$, where χ_M is the corrected molar susceptibility.

Cyclic voltammetry

Cyclic voltammograms were recorded at 298 K on PAR model 370 electrochemistry system consisting of a model 174A polarographic analyzer and a model 175 universal programmer. A standard three-electrode cell was employed with a Beckman M-39273 platinum-inlay working electrode, a platinum-wire auxiliary electrode and a saturated calomel electrode (SCE) as reference; no corrections were made for junction potentials. Details of cell configuration and criterion for reversibility are as reported previously.[17]

Crystallography

Crystal data on **2** and **3** were collected at 293(2) K on a Enraf Nonius MACH2 diffractometer, equipped with graphite-monochromated Mo Kα radiation (λ = 0.71073 Å). Data were corrected for Lorentz and polarization effects. The structures were solved with SIR-92 and refined with the SHELXL-97 package incorporated in the WINGX 1.64 crystallographic collective package.[22] Anisotropic refinements were performed by full-matrix least-squares procedure on F^2. The positions of the hydrogen atoms were calculated assuming ideal geometries, but not refined. All non-hydrogen atoms were refined with anisotropic thermal parameters. The quality of crystals obtained was not very good (high R_{int} values), which could be the reason for higher R values observed. Unfortunately, we could not grow single crystals of **2** and **3** better than the ones used for the present study, as they were the best we could have. Crystal data, data collection, and refinement parameters for **2** and **3** are listed in Table 1.

CCDC reference numbers 209232 (**2**) and 209231 (**3**).

See http://www.rsc.org/suppdata/dt/b3/b305574d/ for crystallographic data in CIF or other electronic format.

Results and discussion

Syntheses

The ligand L^6 was synthesized in high yield by phase-transfer catalysed reactions of 3-(2-pyridyl)pyrazole and 2-chloro-

Table 1 Data collection and structure refinement parameters for $[Co(L^6)_2][ClO_4]_2$ (**2**) and $[Ni(L^6)_2][ClO_4]_2$ (**3**)

	2	**3**
Chemical formula	$C_{28}H_{24}Cl_2CoN_8O_8$	$C_{28}H_{24}Cl_2NiN_8O_8$
M	730.38	730.16
Crystal system	Triclinic	Triclinic
a/Å	11.875(5)	11.930(6)
b/Å	14.540(5)	14.639(8)
c/Å	19.271(5)	19.008(12)
α/°	94.01(5)	93.43(5)
β/°	93.00(5)	92.68(5)
γ/°	112.22(5)	112.07(5)
U/Å^3	3083.3(19)	3062(3)
T/K	293(2)	293(2)
Space group	$P\bar{1}$ (no. 2)	$P\bar{1}$ (no. 2)
Z	4	4
μ(Mo-Kα)/mm^{-1}	0.794	0.872
Unique reflections [R(int)]	8023 [0.1551]	8005 [0.2011]
R^a [$I > 2\sigma(I)$]	0.0745	0.0775
R'^b [$I > 2\sigma(I)$]	0.1445	0.1447

^{a} $R = \Sigma(||F_o| - |F_c||)/\Sigma|F_o|$. ^{b} $R' = \{\Sigma[w(F_o^2 - F_c^2)^2]/\Sigma[w(F_o^2)^2]\}^{1/2}$.

Table 2 Selected bond lengths (Å) and angles (°) for $[Co(L^6)_2]$-$[ClO_4]_2$ (**2**) and $[Ni(L^6)_2][ClO_4]_2$ (**3**)

2		**3**	
Co(1)–N(1a)	2.157(8)	Ni(1)–N(1a)	2.129(11)
Co(1)–N(2a)	2.000(8)	Ni(1)–N(2a)	1.938(11)
Co(1)–N(4a)	2.270(9)	Ni(1)–N(4a)	2.224(11)
Co(1)–N(5a)	2.147(9)	Ni(1)–N(5a)	2.130(11)
Co(1)–N(6a)	2.006(8)	Ni(1)–N(6a)	1.917(12)
Co(1)–N(8a)	2.245(9)	Ni(1)–N(8a)	2.216(11)
Co(2)–N(1b)	2.212(10)	Ni(2)–N(1b)	2.166(18)
Co(2)–N(2b)	2.017(9)	Ni(2)–N(2b)	1.969(13)
Co(2)–N(4b)	2.175(10)	Ni(2)–N(4b)	2.087(14)
Co(2)–N(5b)	2.169(8)	Ni(2)–N(5b)	2.148(11)
Co(2)–N(6b)	2.002(9)	Ni(2)–N(6b)	1.985(13)
Co(2)–N(8b)	2.190(8)	Ni(2)–N(8b)	2.160(11)
N(1a)–Co(1)-(2a)	75.4(4)	N(1a)–Ni(1)–N(2a)	75.0(6)
N(1a)–Co(1)-(4a)	156.8(4)	N(1a)–Ni(1)–N(4a)	160.1(5)
N(2a)–Co(1)-(4a)	84.3(4)	N(2a)–Ni(1)–N(4a)	87.0(5)
N(5a)–Co(1)-(6a)	76.8(4)	N(5a)–Ni(1)–N(6a)	78.1(5)
N(5a)–Co(1)-(8a)	159.1(3)	N(5a)–Ni(1)–N(8a)	161.6(5)
N(6a)–Co(1)-(8a)	85.6(4)	N(6a)–Ni(1)–N(8a)	86.3(6)
N(2a)–Co(1)-(6a)	173.4(4)	N(2a)–Ni(1)–N(6a)	172.8(5)
N(1b)–Co(2)-(2b)	74.4(4)	N(1b)–Ni(2)–N(2b)	74.8(8)
N(1b)–Co(2)-(4b)	158.0(4)	N(1b)–Ni(2)–N(4b)	161.8(7)
N(2b)–Co(2)-(4b)	86.9(4)	N(2b)–Ni(2)–N(4b)	88.9(8)
N(5b)–Co(2)-(6b)	77.1(4)	N(5b)–Ni(2)–N(6b)	77.0(7)
N(6b)–Co(2)-(8b)	83.1(4)	N(6b)–Ni(2)–N(8b)	85.8(6)
N(2b)–Co(2)-(6b)	170.5(5)	N(2b)–Ni(2)–N(6b)	170.7(8)

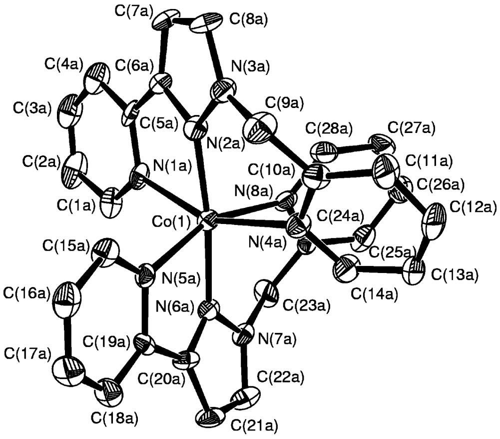

Fig. 1 Perspective view of one crystallographically independent dication in the crystal of $[Co(L^6)_2][ClO_4]_2$ (**2**), showing the atom numbering. Atoms are drawn at the 20% probability level. Hydrogen atoms are omitted for clarity.

methylpyridine hydrochloride under basic conditions. The purity of the ligand was checked by its ^{1}H NMR spectra. The bis-ligand complexes of composition $[M(L^6)_2][ClO_4]_2$ (M = Fe, Co and Ni) were prepared by the straightforward stoichiometric reactions in methanol (in the case of nickel complex the medium was aqueous methanolic) between metal(II) perchlorate hexahydrate and the ligand L^6. In their IR spectra all the complexes display ionic perchlorate bands at ~1100 and ~620 cm^{-1}. In MeCN solution, complexes **1**–**3** behave as 1 : 2 electrolytes. The elemental analyses, IR spectra and solution electrical conductivity data are in good agreement with the proposed formulations. Complexes **2** and **3** have been structurally characterized. Unfortunately, all our attempts to grow single crystals of **1** suitable for crystallographic analysis have been unsuccessful so far. Complexes **1** and **2** are isomorphous by X-ray (see below). Complexes **1**–**3** display closely similar IR spectra (Fig. S1–S3).†

Crystal structures

In order to confirm the structure and mode of co-ordination of the ligand L^6 as well as to determine the chelate ring conformations of the co-ordinated ligands, single crystal X-ray structure determinations of $[Co(L^6)_2][ClO_4]_2$ (**2**) and $[Ni(L^6)_2][ClO_4]_2$ (**3**) were carried out. For both compounds the asymmetric unit contains two crystallographically independent molecules. Both molecules have essentially identical co-ordination geometries, but the corresponding bond lengths and bond angles are slightly different (Table 2). Since the compounds **2** and **3** are essentially isomorphous to get a generalised picture a perspective view of the discrete complex cation in **2** is shown in Fig. 1. The structure of the ligand and its tridentate chelation to the metal are thus confirmed. The non-planar ligand L^6 adopts a *mer* configuration and the two ligands provide a distorted MN$_6$ octahedron about the metal atom. Selected metric parameters associated with the M(II) centre are given in Table 2. Gross distortions from octahedral symmetry are evident in the MN$_6$ core geometry with M–N bond distances and angular deviations from octahedral values (Table 2). There are three types of heterocyclic nitrogen donor atoms; two pyrazole nitrogens [N(2a) and N(6a)], two pyridine rings directly linked with pyrazole rings [N(1a) and N(5a)] and two pyridine rings separated by methylene spacers [N(4a) and N(8a)]. The M–N$_{\text{pyrazole}}$ bond lengths [2.003(8) and 2.010(9) Å for **2**; 1.928(12) and 1.977(13) Å for **3**] are appreciably shorter than the M–N$_{\text{pyridine}}$ bond lengths [pyridine ring directly attached to pyrazole ring: 2.152(9) and 2.191(9) for **2**; 2.130(11) and 2.157(15) Å for **3**; pyridine ring separated by a methylene spacer: 2.258(9) and 2.183(9) for **2**; 2.220(11) and 2.124(13) Å for **3**]. Thus we note for **2** and **3**, the M–N$_{\text{pyridine}}$ (the pyridine ring directly attached to the pyrazole ring) distance is shorter than that of M–N$_{\text{pyridine}}$ (separated by a methylene spacer) distance by ~0.11 /~0.01 Å (**2**) and ~0.09/~0.03 Å (**3**). For $[Ni(L^3)_2][ClO_4]_2$ a similar trend of Ni–N$_{\text{pyrazole}}$ bond distance considerably shorter than that of Ni–N$_{\text{pyridine}}$ was observed.[4a]

For a given ligand the directly attached pyrazole–pyridine unit is almost planar [~3.9° (~ 10.1°) for **2** and ~5.2° (~8.1°) for **3**] and the angles between the pyrazole ring of the pyrazole–pyridine unit and the pyridine ring with a methylene spacer are ~39.8° (~46.9°) for **2** and ~36.7° (~45.2°) for **3**. For a given ligand the pyridine ring of the pyrazole–pyridine unit makes with other pyridine ring an angle of ~39.0° (~39.2°) for **2** and ~35.9° (~38.3°) for **3**, respectively. Thus the six-membered chelate rings exist in boat conformations. Similar chelate ring conformation was observed in the crystal structures of compounds with this class of non-planar ligands.[4,8,10,11]

Absorption spectra

The absorption spectrum of **1** in MeCN at 298 K (Fig. 2) shows a weak absorption at 12 361 cm^{-1}, that is assigned to $^5T_{2g} \longrightarrow {}^5E_g$ transition of an $S = 2$ Fe(II) ion in octahedral symmetry.[7,23] This band is clearly split into two components (the tail of an additional low-intensity absorption in the 10 000–9090 cm^{-1} region could clearly be noticed, which could not be located due to instrumental limitation), due to a combination of a dynamic Jahn–Teller effect in the electronic excited states and a lowering of metal site symmetry.[7,23] It is worth mentioning here that for $[Fe(L^3)_2][ClO_4]_2{\cdot}H_2O$ these bands were observed at 10 741 cm^{-1} and 12 804 cm^{-1}.[7] The band at 24 450 cm^{-1} is due to a MLCT transition, as observed in related systems. Intraligand transitions are seen at still higher energies.

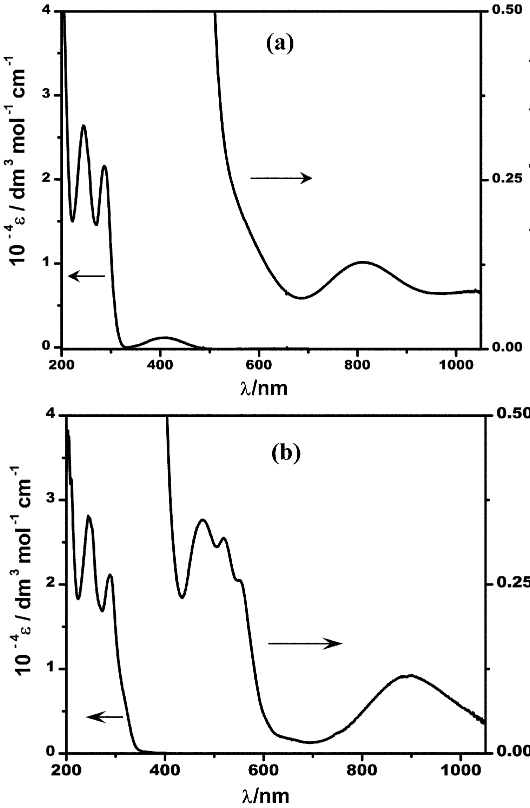

Fig. 2 Electronic spectra of (a) $[Fe(L^6)_2][ClO_4]_2$ (**1**), and (b) $[Co(L^6)_2][ClO_4]_2$ (**2**), in MeCN at 298 K.

The visible spectrum of cobalt(II) complex **2** (Fig. 2) has been assigned[5a,23] and analysed[24] in order to compare the co-ordinating behaviour of L^6 toward six-co-ordinate cobalt(II). Three spin-allowed d–d transitions are expected for octahedral cobalt(II) unless the field strength of the ligands is such that the $^4A_{2g}$ and $^4T_{1g}$ (P) terms have the same energy. This occurs when the two states cross. The assignment of ν_1 (11 087 cm^{-1}) to the $^4T_{1g}$ (F) $\longrightarrow$ $^4T_{2g}$ (F) transition is unequivocal; however, depending upon the D_q/B ratio, ν_2 (20 964 cm^{-1}) may be either $^4T_{1g}$ (F) $\longrightarrow$ $^4T_{1g}$ (P) or $^4T_{1g}$ (F) $\longrightarrow$ $^4A_{2g}$. If ν_2 is assigned to $^4T_{1g}$ (F) $\longrightarrow$ $^4A_{2g}$, then $D_q = \nu_2 - \nu_1/10$; however, the D_q value obtained in this manner (988 cm^{-1}) does not compare well with the nickel(II) value (*vide infra*). If the alternative arrangement is made, then spectral parameters can be calculated by using appropriate equations. The D_q value thus obtained is 1228 cm^{-1}, in reasonable agreement with that obtained with the nickel(II) value of 1149 cm^{-1}. This indicates the correctness of the band assignments and confirms that ν_2 is the transition between the $^4T_{1g}$ states. Intraligand transitions are seen at still higher energies.

The electronic spectrum of nickel(II) complex **3** (Fig. S4) displays $^3A_{2g} \longrightarrow {}^3T_{1g}$ (F) (ν_2) transition at 17 921 cm^{-1}.[5a,7a,9c,23] The D_q value 1149 cm^{-1} has been obtained from $^3A_{2g} \longrightarrow {}^3T_{2g}$ (ν_1) transition. A spin-forbidden transition $^3A_{2g} \longrightarrow {}^1E_g$ (D) (ν') is located at 12 820 cm^{-1}. Following the equations of Dou,[24] the B'_{av} value was calculated as 784 cm^{-1}, which is approximately 70% of the free-ion value (1120 cm^{-1}). This indicates ~30% covalent character in the metal–ligand bonds, which is a significant increase in electron delocalization as compared to the nickel(II) complexes of bidentate ligand L^1 and tridentate ligands L^3 and L^5. It is worth noting here that the D_q values for $[Ni(L^1)_3][ClO_4]_2$, $[Ni(L^3)_2][ClO_4]_2$ and $[Ni(L^5)_2][ClO_4]_2$ were determined to be as 1027, 1152 and 1073 cm^{-1}, respectively; the B'_{av} values were calculated to be 896, 976 and 853 cm^{-1}, respectively.[7a,9c] Intraligand transitions are seen at still higher energies, as expected. Thus we note that the crystal field strength of L^6 towards six-co-ordinate nickel(II) is comparable to the previously reported tridentate ligand L^3 but is appreciably greater than that with complexes with ligands L^1/L^5. Interestingly, the extent of metal–ligand covalency has increased substantially in going from L^1/L^3/L^5 to L^6.

Magnetism

To confirm the spin-state of the iron(II), cobalt(II) and nickel(II) bis-ligand complexes variable temperature magnetic susceptibility measurements were performed on powdered samples using a SQUID magnetometer (complexes **1** and **2**) and the Faraday (complex **3**) method. Thus the temperature-dependence (6–300 K for **1** and **2** and 80–300 K for **3**) of the magnetic susceptibility of solid samples of **1**, **2** and **3** have been measured. The room-temperature values were found to be 5.18, 4.45 and 3.07 μ_B, respectively. These magnetic data clearly establish the high-spin electronic configuration $S = 2$, 3/2 and 1, respectively, of complexes **1**–**3**.[5a,7a,9e] The data for **2** (Fig. S5)[9e] and **3** (Fig. S6) were found to adhere closely to the Curie–Weiss law [$\chi_M = C/(T - \theta)$]. The Curie constants thus obtained [2.56 for **2** and 1.37 for **3**; $C = 1.875$ when $g = 2$ (for $S = 3/2$) and $C = 1$ when $g = 2$ (for $S = 1$)] are in good agreement with that for $S = 3/2$ and 1, respectively. Measurements of magnetic susceptibilities on MeCN solutions at 298 K (Evans's method[20]) of complexes **1**–**3** gave effective magnetic moments, 4.97, 4.65 and 3.05 μ_B, respectively. These values are in reasonable agreement with the corresponding solid-state values.

Six-co-ordinate iron(II) complexes may be diamagnetic, low-spin ($^1A_1$, LS), paramagnetic, high spin ($^5T_2$, HS), or exhibit a temperature-induced LS ↔ HS transition that depends on the relative magnitude of crystal-field strength of the ligand and the mean electron-pairing energy.[3a,25,26] We described that $[Fe(L^3)_2]^{2+}$ shows a temperature-dependent spin-transition, which was identified by variable-temperature magnetic susceptibility and Mössbauer spectral measurements.[7b] We were interested to extend such studies with a new system, and particularly to $[Fe(L^6)_2]^{2+}$, as it is expected that if a nickel(II) complex has a 10 D_q value in the range 11 300–11 900 cm^{-1} (in fact for **3** it is 11 490 cm^{-1}) then the corresponding iron(II) complex such as complex **1** is expected to be a spin-equilibrium complex.[25c] This is remarkably well fulfilled in the case of complex **1**. From this background the variable-temperature (5.2–300 K) magnetic susceptibility studies on **1** were performed using a SQUID magnetometer.

The magnetic property of **1** is presented in Fig. 3, in the form of $\chi_M T$ *vs.* T plot, χ_M being the molar magnetic susceptibility and T the temperature. The data were recorded in both the cooling and warming modes in order to detect a possible hysteresis effect. Both modes gave identical behaviour, without any hysteresis loop. The temperature dependence of the $\chi_M T$ product obtained in the cooling mode is shown here. The magnetic behaviour (Fig. 3) is indicative of the occurrence of a temperature-induced singlet ↔ quintet transition in the $[Fe(L^6)_2]^{2+}$ cation. The $\chi_M T$ value is equal to 3.36 cm^3 mol^{-1} K (a value which corresponds to an effective magnetic moment of

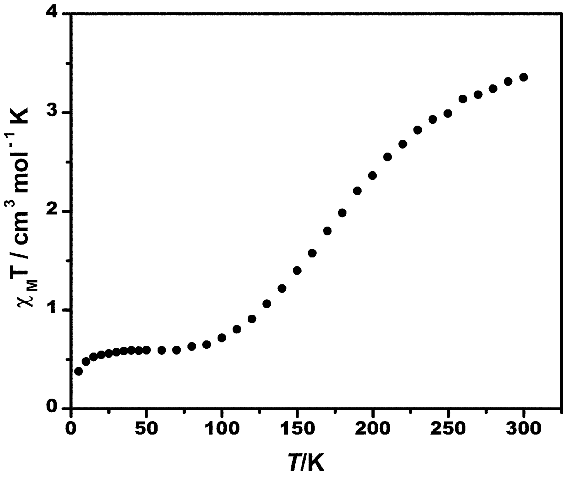

Fig. 3 Temperature dependence of the $\chi_M T$ product for powdered samples of [Fe(L^6)$_2$][ClO$_4$]$_2$ (**1**).

5.18 μ_B) at 300 K and it decreases when cooling to reach a value of 0.59 cm^3 mol^{-1} K (μ_{eff} = 2.18 μ_B) at 70 K and remains almost constant down to 30 K [$\chi_M T$ = 0.57 cm^3 mol^{-1} K (μ_{eff} = 2.14 μ_B)]. Thereafter, it decreases slowly down to 5.2 K [$\chi_M T$ = 0.38 cm^3 mol^{-1} K (μ_{eff} = 1.74 μ_B)]. The magnetic moment value determined at 300 K clearly indicates that the attainment of high-spin (quintet $^5T_2$) state is complete at the highest temperature. The data at the lowest temperature is significantly higher than the temperature-independent paramagnetic value (0.6 μ_B; *vide infra*)[26a] expected for low-spin iron(II) complexes. The μ_{eff} value at 5.2 K provides evidence for the existence of residual amount of high-spin molecules in the predominantly low-spin form at low temperatures. The $\chi_M T$ value indicates the presence of ~10% of paramagnetic high-spin species in the low-spin matrix.

The equilibrium between the two electronic states is analysed with the equilibrium constant determination K_{eq} for the equilibrium [$^1A_1$ (ls) ↔ $^5T_2$ (hs)]. The high-spin to low-spin fraction ratio K_{eq} is determined from eqn (1),[26b]

$$K_{eq} = m_{hs}/m_{ls} = (\mu_{exptl}^2 - \mu_{ls}^2)/(\mu_{hs}^2 - \mu_{exptl}^2) \qquad (1)$$

where μ_{exptl} is the experimentally determined magnetic moment at a given temperature, m_{ls} is the mole fraction of the low-spin form and m_{hs} is that of the high-spin form, μ_{ls} and μ_{hs} are the effective magnetic moments for the low-spin and high-spin forms. In these calculations μ_{hs} was taken as 5.2 μ_B and μ_{ls} was taken as 0.6 μ_B to take account of the temperature-independent paramagnetism. In fact for a closely related complex [Fe(L^3)$_2$][ClO$_4$]$_2$ which displayed temperature-induced spin transition the experimentally determined value was 0.6 μ_B at 10 K and for [Fe(L^5)$_2$][ClO$_4$]$_2$ the value of μ_{hs} at 300 K was determined to be 5.2 μ_B.[7b] The ln K_{eq} *vs.* 1/T relationship is linear to a good approximation over the temperature range 190–250 K (Fig. 4). In this case, it is possible to get an estimate of ΔH and ΔS (which include electronic and molecular vibrational contributions).[25] The thermodyanamic parameters derived from this straight line were ΔH = 9.7 kJ mol^{-1} and ΔS = 56 J K^{-1} mol^{-1}. These values are in reasonable agreement with those obtained other six-co-ordinate Fe(II) compounds.[25a] The source of the ΔH is the Fe–N bond length increase, which accompanies the transition from low to high spin, *i.e.*, reorganization of the inner co-ordination sphere.[25a,b] The entropy term cannot be explained solely by the spin multiplicity change.[25a,26a] Measured values of the entropy changes at high-spin ↔ low-spin transitions for complexes of iron(II) vary between about 48 and 86 J K^{-1} mol^{-1}.[25a] This is considerably more than the value expected for a change in spin state alone (R ln 5 = 13.4 J K^{-1} mol^{-1}).[25,26] The excess no doubt mainly arises from the changes in the vibrational characteristics of the co-ordination core and the lattice. It should be noted here that for [Fe(L^3)$_2$][ClO$_4$]$_2$·H$_2$O the thermodynamic parameters obtained were ΔH = 13 kJ mol^{-1} and ΔS = 56 J K^{-1} mol^{-1}.[7b]

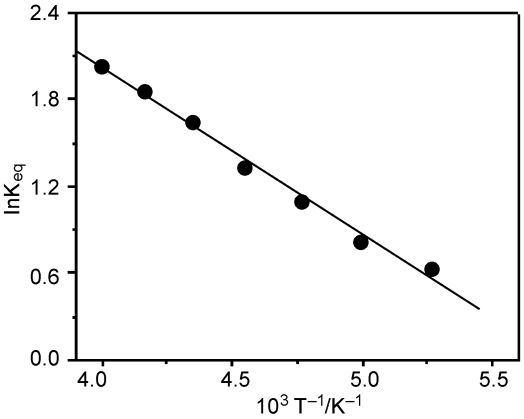

Fig. 4 Plot of ln K_{eq} [$^1A_1$ (ls)↔$^5T_2$ (hs)] *vs.* 1/T between 190–250 K for [Fe(L^6)$_2$][ClO$_4$]$_2$ (**1**).

Redox properties

The redox behaviour of complexes **1**–**3** has been studied by cyclic voltammetry (CV). We consider first the behaviour of iron(II) complex **1**. The CV scan at a scan rate of 100 mV s^{-1} (Fig. 5) displays a small inflection at 0.62 V and an oxidative response at 1.06 V *vs.* SCE. During the reverse (cathodic) scan an ill-defined wave is clearly observable at 0.88 V, with an additional reductive wave at 0.26 V *vs.* SCE. The nature of the response remains invariant to increase in the scan rate (200 and 500 mV s^{-1}) and repetitive scanning between this potential window (0.0 to 1.6 V). We believe that change in the spin-state properties of Fe(II) and Fe(III) is the reason for the observed effect. It is reasonable to assume, due to presence of directly attached pyrazole–pyridine moiety, that L^6 would stabilize low-spin state of Fe(III). It is worth noting here that, where such a possibility does not exist, the complex [Fe(L^3)$_2$][ClO$_4$]$_2$·H$_2$O exhibited a reversible Fe^{III}/Fe^{II} redox process: $E_{1/2}$ = 1.06 V *vs.* SCE and ΔE_p = 80 mV.[7a] Further studies are on to underpin the cause of irreversible redox behaviour of **1**. The behaviour of

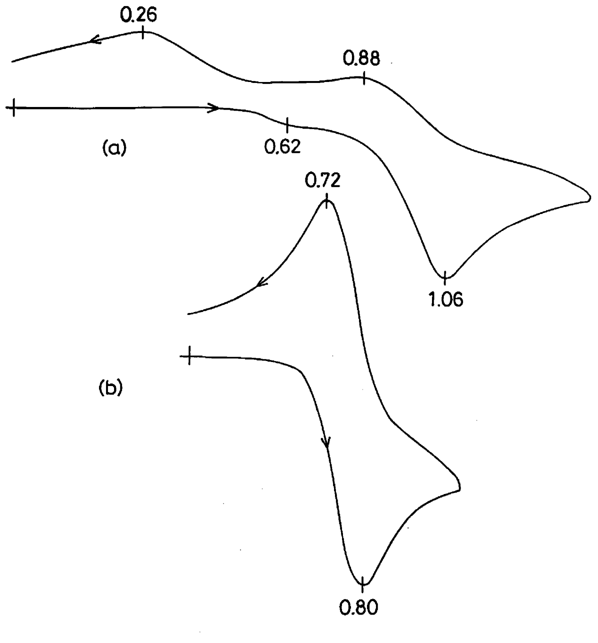

Fig. 5 Cyclic voltammograms of (a) [Fe(L^6)$_2$][ClO$_4$]$_2$ (**1**), and (b) [Co(L^6)$_2$][ClO$_4$]$_2$ (**2**), in MeCN. Experimental conditions: supporting electrolyte, 0.1 mol dm^{-3} [NBu$^n_4$][ClO$_4$]; working electrode: platinum; [complex] ≈ 10^{-3} mol dm^{-3}; temperature 25 °C.

cobalt(II) complex **2** is displayed in Fig. 5. The one-electron nature of the redox response of **2** has been confirmed by comparison of current height with the response of samples of $[Co(L^3)_2][ClO_4]_2 \cdot 2H_2O$, under the same experimental conditions.[9e] The reversible wave ($\Delta E_p = 80$ mV)[17] is ascribed to the Co^{III}/Co^{II} couple. The $E_{1/2}$ value is 0.02 V more anodic than that of $[Co(L^3)_2][ClO_4]_2 \cdot 2H_2O$, indicating that the L^6 stabilizes the cobalt(II) toward oxidation. We are not in a position to provide an explanation for the observed reversible redox behaviour of **2**, as it is expected to cause more structural changes in going from a high-spin cobalt(II) to a low-spin cobalt(III). Interestingly, $[Co(L^3)_2][ClO_4]_2 \cdot 2H_2O$ exhibited a reversible Co^{III}/Co^{II} redox process: $E_{1/2} = 0.74$ V *vs.* SCE and $\Delta E_p = 80$ mV.[9e] Complex **3** is electro-inactive in the potential range −1.0 to 1.0 V *vs.* SCE.

Conclusion

This research has resulted in the synthesis of a new ligand based on condensation between 3-(2-pyridyl)pyrazole and 2-picolyl chloride. This new tridentate ligand L^6 co-ordinates to iron(II), cobalt(II) and nickel(II) forming distorted octahedral bis-ligand complexes, the cobalt(II) and nickel(II) complexes are structurally characterized. Due to the weak field nature of this new ligand, as revealed by the analysis of crystal field transitions, these complexes are uniformly high-spin at room temperature (300 K). Interestingly, the iron(II) complex displays in the solid-state anomalous magnetic properties which are associated with a thermally driven singlet ($^1A_1$) ↔ quintet ($^5T_2$) transition. From the linear ln K_{eq} [$^1A_1$ (ls) ↔ $^5T_2$ (hs)] *vs.* $1/T$ relationship (190–250 K), thermodyanamic parameters were then derived. While iron(II) displays in MeCN an irreversible M^{III}/M^{II} redox process for cobalt(II) complex such a redox process is reversible.

A detailed study of the redox behaviour, in conjunction with EPR spectral observations, of complexes **1** and **2** and iron(II) and cobalt(II) complexes of L^3 is planned. Our efforts are being employed to develop the interesting co-ordination chemistry of L^6 towards other metal ions and to the design of new non-planar pyrazolylmethylpyridine heterocyclic ligands.

Acknowledgements

Financial assistance received from the Department of Science and Technology (DST) and the Council of Scientific & Industrial Research (CSIR), Government of India is gratefully acknowledged. We acknowledge the National Single Crystal Diffractometer Facility at this Department for data collection of **2** and **3**. R. M. gratefully acknowledges the award of a joint collaborative grant funded by the Volkswagen Foundation, Germany and the donation of a HP 8453 diode-array spectrophotometer with accessory (Agilent Technologies) through this grant. J. M. gratefully acknowledges the award of a fellowship by CSIR. We specially thank Mr. V. Balamurugan for his help in X-ray structural work. Comments of referees were very helpful at the revision stage.

References

1 (*a*) R. Mukherjee, *Coord. Chem. Rev.*, 2000, **203**, 151 and references therein; (*b*) S. Trofimenko, *Scorpionates – The Coordination Chemistry of Polypyrazolylborate Ligands*, Imperial College Press, London, 1999.
2 R. Mukherjee, *Comprehensive Coordination Chemistry-II: From Biology to Nanotechnology*, Pergamon, 2003, vol. 5, in press.
3 (*a*) J. M. Holland, J. A. McAlister, C. A. Kilner, M. Thornton-Pett, A. J. Bridgeman and M. A. Halcrow, *J. Chem. Soc., Dalton Trans.*, 2002, 548 and references therein; (*b*) C. L. Foster, C. A. Kilner, M. Thornton-Pett and M. A. Halcrow, *Polyhedron*, 2002, **21**, 1031.
4 (*a*) A. A. Watson, D. A. House and P. J. Steel, *Inorg. Chim. Acta*, 1987, **130**, 167; (*b*) D. A. House, P. J. Steel and A. A. Watson, *Aust. J. Chem.*, 1986, **39**, 1525.
5 (*a*) T. K. Lal and R. Mukherjee, *Polyhedron*, 1997, **16**, 3577; (*b*) T. K. Lal, J. F. Richardson, M. S. Mashuta, R. M. Buchanan and R. Mukherjee, *Polyhedron*, 1997, **16**, 4331; (*c*) T. K. Lal, R. Gupta, S. Mahapatra and R. Mukherjee, *Polyhedron*, 1999, **18**, 1743; (*d*) R. Gupta, T. K. Lal and R. Mukherjee, *Polyhedron*, 2002, **21**, 1245.
6 Z. Shirin, R. Mukherjee, J. F. Richardson and R. M. Buchanan, *J. Chem. Soc., Dalton Trans.*, 1994, 465.
7 (*a*) S. Mahapatra, N. Gupta and R. Mukherjee, *J. Chem. Soc., Dalton Trans.*, 1991, 2911; (*b*) S. Mahapatra and R. Mukherjee, *Polyhedron*, 1993, **12**, 1603.
8 (*a*) S. Mahapatra, R. J. Butcher and R. Mukherjee, *J. Chem. Soc., Dalton Trans.*, 1993, 3723; (*b*) S. Mahapatra, R. J. Butcher and R. Mukherjee, *Indian J. Chem.*, 2001, **40A**, 973.
9 (*a*) S. Mahapatra, D. Bhuniya and R. Mukherjee, *Polyhedron*, 1992, **11**, 2045; (*b*) S. Mahapatra and R. Mukherjee, *J. Chem. Soc., Dalton Trans.*, 1992, 2337; (*c*) S. Mahapatra and R. Mukherjee, *Indian J. Chem., Sect. A*, 1993, **32**, 64; (*d*) S. Mahapatra and R. Mukherjee, *Indian J. Chem., Sect. A*, 1993, **32**, 428; (*e*) S. Mahapatra, T. K. Lal and R. Mukherjee, *Polyhedron*, 1993, **12**, 1477; (*f*) R. Gupta and R. Mukherjee, *Polyhedron*, 2001, **20**, 2545.
10 (*a*) P. Manikandan, B. Varghese and P. T. Manoharan, *J. Chem. Soc., Dalton Trans.*, 1996, 371; (*b*) P. Manikandan, K. R. Justin Thomas and P. T. Manoharan, *Acta Crystallogr., Sect. C*, 2000, **56**, 308; (*c*) P. Manikandan, K. R. Justin Thomas and P. T. Manoharan, *J. Chem. Soc., Dalton Trans.*, 2000, 2779; (*d*) P. Manikandan, R. Muthukumaran, K. R. Justin Thomas, B. Varghese, G. V. R. Chandramouli and P. T. Manoharan, *Inorg. Chem.*, 2001, **40**, 2378.
11 K. G. Orrell, A. G. Osborne, M. W. da Silva, M. B. Hursthouse and S. J. Coles, *Polyhedron*, 1997, **16**, 3003.
12 (*a*) Y. Lin and S. A. Lang, jr., *J. Heterocycl. Chem.*, 1977, **14**, 345; (*b*) A. J. Amoroso, A. M. C. Thompson, J. C. Jeffery, P. L. Jones, J. A. McCleverty and M. D. Ward, *J. Chem. Soc., Chem. Commun.*, 1994, 2751.
13 M. D. Ward, J. A. McCleverty and J. C. Jeffery, *Coord. Chem. Rev.*, 2001, **222**, 251.
14 P. L. Jones, A. J. Amoroso, J. C. Jeffery, J. A. McCleverty, E. Psillakis, L. H. Rees and M. D. Ward, *Inorg. Chem.*, 1997, **36**, 10; P. L. Jones, J. C. Jeffery, J. A. McCleverty and M. D. ward, *Polyhedron*, 1997, **16**, 1567; J. S. Fleming, K. L. V. Mann, C.-A. Carraz, E. Psillakis, J. C. Jeffery, J. A. McCleverty and M. D. Ward, *Angew. Chem., Int. Ed.*, 1998, **37**, 1279; K. L. V. Mann, E. Psillakis, J. C. Jeffery, L. H. Rees, N. M. Harden, J. A. McCleverty, M. D. Ward, D. Gatteschi, F. Totti, F. E. Mabbs, E. J. L. McInnes, P. C. Riedi and G. M. Smith, *J. Chem. Soc., Dalton Trans.*, 1999, 339; R. L. Paul, S. M. Couchman, J. C. Jeffery, J. A. McCleverty, Z. R. Reeves and M. D. Ward, *J. Chem. Soc., Dalton Trans.*, 2000, 845; Z. R. Bell, J. C. Jeffery, J. A. McCleverty and M. D. Ward, *Angew. Chem., Int. Ed.*, 2002, **41**, 2515.
15 D. A. McMorran and P. J. Steel, *Chem. Commun.*, 2002, 2120.
16 W. R. Thiel and T. Priermeier, *Angew. Chem., Int. Ed.*, 1995, **34**, 1737; H. Glas, E. Herdtweck, G. R. J. Artus and W. R. Thiel, *Inorg. Chem.*, 1998, **37**, 3644.
17 N. Gupta, S. Mukerjee, S. Mahapatra, M. Ray and R. Mukherjee, *Inorg. Chem.*, 1992, **31**, 139.
18 W. J. Geary, *Coord. Chem. Rev.*, 1971, **7**, 81.
19 R. Gupta, S. Mukherjee and R. Mukherjee, *J. Chem. Soc., Dalton Trans.*, 1999, 4025 and references therein.
20 D. F. Evans, *J. Chem. Soc.*, 1959, 2003.
21 C. J. O'Connor, *Prog. Inorg. Chem.*, 1982, **29**, 203.
22 L. J. Farrugia, WINGX ver 1.64, An Integrated Systems of Windows programs for the Solution, Refinement, and Analysis of single-crystal X-ray diffraction data, Department of Chemistry, University of Glasgow, 2003.
23 F. A. Cotton, G. Wilkinson, C. A. Murillo and M. Bochmann, *Advanced Inorganic Chemistry*, Wiley, New York, 6th edn., 1999.
24 Y.-S. Dou, *J. Chem. Educ.*, 1990, **67**, 134.
25 (*a*) E. König, G. Ritter and S. K. Kulshreshtha, *Chem. Rev.*, 1985, **85**, 219; (*b*) E. König, *Prog. Inorg. Chem.*, 1987, **35**, 527; (*c*) H. Toftlund, *Coord. Chem. Rev.*, 1989, **94**, 67.
26 (*a*) M. J. Boylan, S. M. Nelson and F. A. Deeney, *J. Chem. Soc. A*, 1971, 976; (*b*) K. A. Reeder, E. V. Dose and L. J. Wilson, *Inorg. Chem.*, 1978, **17**, 1071; (*c*) B. Gallois, J.-A. Real, C. Hauw and J. Zarembowitch, *Inorg. Chem.*, 1990, **29**, 1152; (*d*) J. A. Real, M. C. Muñoz, E. Andrés, T. Granier and B. Gallois, *Inorg. Chem.*, 1994, **33**, 3587.